Published in final edited form as:
Nat Cell Biol. 2013 October ; 15(10): . doi:10.1038/ncb2843.

In vivo reprogramming of astrocytes to neuroblasts in the adult brain

Wenze Niu[1], **Tong Zang**[1], **Yuhua Zou**[1], **Sanhua Fang**[1,2], **Derek K. Smith**[1], **Robert Bachoo**[3], and **Chun-Li Zhang**[1,4]

[1]Department of Molecular Biology, University of Texas Southwestern Medical Center, 6000 Harry Hines Boulevard, Dallas, Texas 75390, USA

[2]Department of Pharmacology and Institute of Neuroscience, School of Medicine, Zhejiang University, 866 Yuhangtang Road, Hangzhou, Zhejiang 310058, China

[3]Department of Neurology, University of Texas Southwestern Medical Center, 6000 Harry Hines Boulevard, Dallas, Texas 75390, USA

Abstract

Adult differentiated cells can be reprogrammed into pluripotent stem cells or lineage-restricted proliferating precursors in culture; however, this has not been demonstrated *in vivo*. Here, we show that the single transcription factor SOX2 is sufficient to reprogram resident astrocytes into proliferative neuroblasts in the adult mouse brain. These induced adult neuroblasts (iANBs) persist for months and can be generated even in aged brains. When supplied with BDNF and noggin or when the mice are treated with a histone deacetylase inhibitor, iANBs develop into electrophysiologically mature neurons, which functionally integrate into the local neural network. Our results demonstrate that adult astrocytes exhibit remarkable plasticity *in vivo*, a feature that might have important implications in regeneration of the central nervous system using endogenous patient-specific glial cells.

Neural stem cells (NSCs) persist mainly in two discrete regions of the adult central nervous system (CNS): the subgranular zone of the dentate gyrus and the subventricular zone (SVZ) of the lateral ventricle. These adult NSCs give rise to doublecortin (DCX)-positive neuroblasts, which further differentiate into mature neurons that integrate into local circuitry within the dentate gyrus or olfactory bulbs[1–6]. In response to injury, neuroblasts from the SVZ exhibit limited migration to nearby damaged regions and differentiate into specific neural lineages[7–9]. These events clearly demonstrate the cellular and structural plasticity of neural networks in the adult brain and establish a theoretical foundation for cell regeneration-based therapies of CNS diseases. One limitation to this approach is the confinement of robust neurogenesis to the adult subgranular zone and SVZ thus limiting the therapeutic potential of native NSCs.

[4]Correspondence should be addressed to C.L.Z., Chun-Li.Zhang@UTSouthwestern.edu.

AUTHOR CONTRIBUTIONS

W.N., T.Z. and C-L.Z. conceived and designed the experiments. W.N., T.Z., Y.Z. and C-L.Z. performed experiments. S.F. contributed to partial surgical experiments. D.K.S. critically reviewed and edited the manuscript. R.B. developed the *Cst3–CreER*^{T2} transgenic mice. W.N., T.Z. and C-L.Z. analysed data and prepared the manuscript.

COMPETING FINANCIAL INTERESTS

The authors declare no competing financial interests.

Lineage reprogramming provides an avenue towards cellular regeneration. Differentiated cells in culture have been reprogrammed into pluripotent stem cells and lineage-restricted precursors[10–15]. Fibroblasts, astrocytes or pericytes can be converted to postmitotic neurons *in vitro*[16–22]. Further, direct cell fate conversion was demonstrated in adult mice by transcription-factor-mediated reprogramming of pancreatic exocrine cells to β-cells and cardiac fibroblasts to cardiomyocytes[23–25]. A recent report also showed the potential of direct neuronal conversion *in vivo*[26]. Notwithstanding, it remains unclear whether differentiated cells can be *in vivo* reprogrammed to proliferating precursors.

Astrocytes are the most abundant and ubiquitously distributed non-neuronal cells in the adult CNS. They become reactive and form glial scars in response to damage or neurodegeneration. These glial scars are initially beneficial for restricting damage spread but ultimately hinder axonal regeneration[27–29]. Therefore, these glial cells might be an ideal target for *in vivo* neuronal conversion after neural injury. Previous studies demonstrate that early postnatal mouse astrocytes can be directly converted into neurons or stem-like cells by the forced expression of a single transcription factor *in vitro*[18,19,30], highlighting the plasticity of these somatic glial cells. Here, we demonstrate that the single transcription factor SOX2 is capable of converting resident astrocytes into proliferative neuroblasts, which further develop into functionally mature neurons *in vivo*.

RESULTS

Induction of neuroblasts in the adult mouse striatum

We used a lentiviral delivery system to target astrocytes in adult mouse striatum. Striatum was chosen owing to its large, distinctive structure that facilitates viral injection. Gene expression was controlled using a synthetic promoter and enhancer derived from the human glial fibrillary acidic protein (*hGFAP*) gene[31]. Using green fluorescent protein (GFP) as a control, robust expression was detected along the needle track in adult striatum at 1 week and 4 weeks post viral injection (wpi). Of the infected cells, 84% expressed the astrocyte-specific marker GFAP (Supplementary Fig. S1). GFP expression in other cell types was minimal and no DCX expression was detected along or surrounding the injection sites, indicating an absence of neuroblasts in the adult mouse striatum.

Eight transcription factors (ASCL1, BRN2, KLF4, MYC, MYT1L, OCT4, SOX2 and ZFP521) and four microRNAs (*miR9*, *miR124*, *miR125* and *miR128*) were chosen as candidates on the basis of their known roles in stem cell maintenance or neurogenesis. Lentiviruses encoding these 12 factors were subdivided into 3 mini-pools and bilaterally injected into the striatum of adult mice. Injection sites were selected far from the lateral ventricle (>1,000 μm) to prevent aberrant detection of cells potentially originating from the neurogenic niche (Fig. 1a). Brain sections were stained for GFP and DCX at 4 wpi. DCX^+ cells were undetected in striatal regions injected with GFP or two mini-pools of eight total genes (Fig. 1b). Remarkably, robust DCX^+ cells were observed along the needle track in brains injected with a pool of four transcription factors (4F: OCT4, SOX2, MYC and KLF4), a combination previously used to induce pluripotent stem cells[10]. These DCX^+ cells showed typical bipolar or multipolar processes that resembled the morphology of neuroblasts or immature neurons (Fig. 1c). These cells also expressed PSA-NCAM, another marker for neuroblasts[32] (Fig. 1d). Furthermore, DCX^+ cells were labelled by repetitive bromodeoxyuridine (BrdU) administration, indicating that they were newly produced (Fig. 1e). Owing to the immature and proliferative nature of these DCX^+ cells, we designated them as iANBs. Interestingly, 4F-induced iANBs were identified in mice across several age groups (Fig. 1f).

SOX2 is necessary and sufficient to generate iANBs

To tease out the essential factor(s) within the 4F pool, we first conducted screens by removing one factor from the pool (4F-1). The elimination of SOX2 completely abolished the generation of iANBs, whereas the exclusion of OCT4, MYC or KLF4 had a minimal effect on iANB induction (Fig. 1g). Unexpectedly, SOX2 alone was sufficient to induce DCX^+ cells with 10-fold greater efficiency than 4F (Fig. 1g,h,j). These DCX^+ cells localized to the needle track with confined local spread (Fig. 1h). In contrast, neither KLF4 nor MYC alone produced any iANBs. OCT4 injections yielded comparably few DCX^+ cells (Fig. 1g).

iANBs were generated in a time-dependent manner with minimal conversion detected 1–3 wpi and peak reprogramming 7 wpi (Fig. 2a–c). Importantly, iANBs persisted beyond 14 wpi, indicating that SOX2 promoted a stable, non-transient induction of these neuroblasts (Fig. 2b). These later generated DCX^+ cells exhibited an increased number of processes and some clustered with neuroblast morphology (Fig. 2c). Moreover, SOX2 successfully induced DCX^+ cells in mice up to 24 months of age, albeit with fivefold reduced efficiency (Fig. 2d–f).

Gene expression under the *hGFAP* promoter is dynamic: high in astrocytes but rarely expressed in neuronal cells (Supplementary Fig. S1). To determine the effect of continual expression of ectopic SOX2 on iANBs, we expressed SOX2 under a constitutively active *CAG* promoter (Supplementary Fig. S2a). Lentivirus-mediated expression of SOX2 was confirmed by immunostaining (Supplementary Fig. S2b). When compared with *hGFAP*–SOX2, *CAG*–SOX2 induced approximately 37-fold fewer DCX^+ cells (Supplementary Fig. S2c). These DCX^+ cells lacked elaborate neuronal morphology, seemed unhealthy and maintained strong SOX2 expression when examined at 5 wpi (Supplementary Fig. S2d,e). In sharp contrast, SOX2 expression in DCX^+ cells induced by *hGFAP*–SOX2 was greatly reduced in a time-dependent manner (Supplementary Fig. S2e). These data indicate that DCX^+ cells are directly derived from SOX2-expressing cells but the constitutive expression of SOX2 is not necessary and might even be detrimental to iANB expansion and survival.

iANBs are locally reprogrammed

Injury and neurodegeneration prompt the migration of neuroblasts from the lateral ventricle to nearby damaged regions[7–9]. To exclude the possibility that DCX^+ cells from the lateral ventricle migrated into the region surrounding the injection site, we analysed striatal regions from GFP control injections for neuroblast markers. No DCX^+ cells were present in or surrounding the injection site following GFP expression (Fig. 1b,h,i). Further, lentiviral expression of GFP–T2A–SOX2 under the *hGFAP* promoter was employed to explicitly identify SOX2-infected cells using a co-expressed GFP marker (Fig. 3a). A complete examination of serial sections through the injected area 7 wpi revealed that GFP signal was undetectable within and surrounding the lateral ventricle (Fig. 3b). This eliminates the possibility that cells in this region were infected. In contrast, SOX2-induced DCX^+ cells were exclusively observed in the injected striatal regions (Fig. 3c–e). All induced DCX^+ cells were co-labelled with GFP, validating that iANBs originate from locally infected cells and not migrating progenitors from the lateral ventricle (Fig. 3d,e).

To further confirm that the induction of iANBs in the striatum is independent of NSC migration from the endogenous neurogenic niches, *Nes–CreER^{TM}* mice[33] were crossed with *Rosa–YFP* reporter mice to label NSCs and their progeny in the lateral ventricle (Fig. 3f,g). SOX2 lentivirus was injected into the striatum nine weeks after tamoxifen induction. DCX^+ cells were co-labelled with yellow fluorescent protein (YFP) in the lateral ventricle, indicating that they were derived from the NSCs (Fig. 3h,i). In stark contrast, no SOX2-

induced DCX^+ cells were co-labelled with YFP in the striatum, suggesting that these cells were locally reprogrammed (Fig. 3j).

iANBs originate from resident astrocytes

Most cells transduced by lentivirus under the *hGFAP* promoter are astrocytes (Supplementary Fig. S1), indicating a potential astrocyte origin of iANBs. To test this hypothesis, we performed a series of lineage-tracing experiments. *Rosa–YFP* reporter mice were crossed with *hGFAP–Cre* mice, which broadly label astrocytes, neurons and oligodendrocytes[34] (Fig. 4a–d). SOX2 injection into the adult *hGFAP–Cre;Rosa–YFP* mice yielded DCX^+ cells with immature neuronal morphology at 5 wpi (Fig. 4e). All of these DCX^+ cells co-labelled with YFP, indicating derivation from the *hGFAP–Cre* lineage.

The broad activity of *hGFAP–Cre* limited its use as an effective tool for identifying the precise cellular origin of iANBs. Recently, astrocyte-specific GFAP expression was demonstrated with the *mGfap–Cre* transgenic line 77.6 (ref. 35). In pursuit of a more rigorous model system, we crossed these mice with a *Rosa–YFP* reporter line and confirmed astrocyte-specific Cre activity. Approximately 98% of YFP^+ cells were co-labelled with the astrocyte marker glutamine synthetase (GS) in the adult striatum (Fig. 4f–i). At 10 weeks of age, the *mGfap–Cre;Rosa–YFP* mice were injected with SOX2-expressing lentivirus. DCX^+ cells were robustly detected in injected striatal regions after 5 weeks and all were YFP^+, indicating an astrocyte-specific lineage (Fig. 4j).

Next, we employed an inducible reporter system as a third approach to confirm the astrocytic origin of iANBs. Cystatin C (Cst3) is enriched in adult astrocytes throughout the brain[36]. *CreER^{T2}* transgenic mice, generated from a BAC clone containing the *Cst3* gene, were crossed with *Rosa–YFP* reporter mice and treated with tamoxifen at 8 weeks of age. YFP^+ cells were widely distributed throughout the brain. Although endogenous *Cst3* is expressed in certain neurons under pathological conditions[37–39], neither neurons nor oligodendrocytes were traced by YFP in the striatum of adult *Cst3–CreER^{T2};Rosa–YFP* mice (Fig. 5a–d). In contrast, immunohistochemical analysis confirmed that 95% of YFP^+ cells are GS^+ or $Aldoc^+$ with an astrocytic morphology in the adult striatum (Fig. 5a–c). The remaining YFP^+ cells stained positive for IBA1, a marker specific to microglia. The physiological properties of *Cst3–CreER^{T2}*-traced cells were examined by whole-cell patch-clamp recording using a *Rosa*–tdTomato (tdT) reporter bright enough for live-cell imaging (Fig. 5e). With the exception of one tdT^+ cell that exhibited a low resting membrane potential (~−23.3 mV) and a high input resistance (~1,000 MΩ) similar to microglia[40], the electrophysiological properties for all of the remaining tdT^+ cells resembled those of a heterogeneous population of astrocytes[41] (Supplementary Fig. S3). No action potentials were elicited following current injections among all of the recorded cells (13 of 13, Fig. 5f). These cells exhibited large potassium currents but no sodium currents were evoked by step voltages (Fig. 5g). Further, all tdT^+ cells (13 of 13) lacked any spontaneous synaptic currents at the resting potential (Fig. 5h). When patched cells were loaded with biocytin, several neighbouring astrocytes were also labelled through gap junction coupling (Fig. 5i). These are stereotypical characteristics of astrocytes[42]. Next, SOX2 or GFP control lentivirus was injected 2 weeks post tamoxifen treatment (Fig. 5j). DCX^+ cells were efficiently induced only in brains injected with SOX2 lentivirus and most clearly co-labelled with YFP (Fig. 5k). These data indicate that $Cst3^+$ astrocytes are the cellular origin of iANBs because the lentiviral *hGFAP* promoter does not drive gene expression in $IBA1^+$ microglia (Supplementary Fig. S1).

We also specifically examined whether iANBs originate from NG2-glia, which are broadly distributed throughout the adult brain and serve as oligodendrocyte precursors[43]. Their lineage was traced with BAC transgenic *NG2–Cre* (ref. 44) and *Rosa–YFP* reporter lines

(Fig. 6a,b). In the core striatal regions, 41% of YFP^+ cells expressed NG2, 46% expressed PDGFRa and 38% expressed Olig2, whereas the markers for astrocytes (GFAP or GS), microglia (IBA1) and mature neurons (NeuN) were rarely or not detected (Fig. 6c,d). Adult mice injected with SOX2 lentivirus exhibited robust induction of DCX^+ cells at 5 wpi, although no cells were co-labelled with YFP, excluding an NG2-glia origin (Fig. 6e).

Some neurons were also transduced with lentivirus and a fraction expressed genes under the *hGFAP* promoter (Supplementary Fig. S1). Although unlikely, this raised a possibility that neurons expressing ectopic SOX2 might undergo dedifferentiation, re-enter the cell cycle, and become DCX^+ neuroblasts. Once again, we examined this possibility with genetic lineage tracing using *PrP–CreER^T;Rosa–tdT* reporter mice[45–47] (Fig. 6f,g). After 8 days of tamoxifen treatment, 82.9% of $NeuN^+$ striatal neurons were tdT^+ and 99% of tdT^+ cells were $NeuN^+$, indicating highly efficient and specific tracing of striatal neurons (Fig. 6h,i). Two weeks post tamoxifen treatment, SOX2-expressing lentivirus was injected into the striatum to induce neuroblasts. At 5 wpi, no cells from a population of 1,032 DCX^+ cells were labelled by tdT, strongly supporting a non-neuronal origin of iANBs (Fig. 6j).

Taken together, these data conclusively demonstrate that SOX2-induced iANBs mainly originate from local mature astrocytes but not from NG2-glia or neurons in the adult striatum.

iANBs pass through a proliferative state

iANBs might be derived from proliferating or quiescent astrocytes because lentivirus transduces both dividing and non-dividing cells. To delineate between these possibilities, we traced actively dividing astrocytes at the time of virus infection by retroviral expression of Cre recombinase using the *hGFAP* promoter in *Rosa–YFP* reporter mice (Fig. 7a,b), because retrovirus targets only actively proliferating cells. Five weeks following retroviral and lentiviral co-injection, only 0.9% of the analysed 3,500 SOX2-induced DCX^+ cells were YFP^+. This indicates that only a small fraction of iANBs originated from proliferating astrocytes at the time of viral infection (Fig. 7c). A detailed analysis of proliferating cells in the adult striatum showed that mature astrocytes rarely proliferate until 3 days after the appearance of injection-induced lesions (Supplementary Fig. S4). These astrocytes could not be targeted by retrovirus injected 3 days earlier because the half-life of infectivity for a retrovirus is 5–8 h at 37 °C (ref. 42). Therefore, comparatively few DCX^+ cells could be generated from proliferative astrocytes transduced with retrovirus. Together, these data show that iANBs can be converted from dividing astrocytes, although most iANBs are derived from quiescent astrocytes.

To determine whether iANBs entered a proliferative stage following reprogramming, the continuous addition of BrdU to drinking water was used to label proliferating cells over a 4-week period beginning one week after SOX2 injection. At 5 wpi, 98.5% of DCX^+ cells were co-labelled with BrdU (Fig. 7d–f). Alternatively, mice receiving two BrdU pulses within 2 h of being euthanized exhibited clustered DCX^+BrdU^+ cells with a co-labelling frequency of 3%. (Fig. 7f). Cell proliferation was further examined by Ki67 staining. Between 4 and 14 wpi, 10–26% of clustered and fewer than 3% of dispersed DCX^+ cells were $Ki67^+$ (Fig. 7g,h). These results indicate that SOX2-reprogrammed iANBs pass through a proliferative stage. Importantly, no tumour formation was observed in any mouse injected with SOX2-expressing lentivirus up to 50 wpi, the longest period examined.

iANBs mature into functional neurons

The cellular fate of proliferating iANBs was evaluated by labelling with BrdU and the neuron-specific nuclear protein NeuN. $BrdU^+NeuN^+$ cells were sparsely distributed in

SOX2-infected mice, which received intraperitoneal injections of BrdU during weeks 4–8 post SOX2 injection (Fig. 8a,b). To eliminate the possibility that daily BrdU injections incompletely labelled iANBs, a second cohort of mice was provided BrdU-containing drinking water for a 4-week period beginning 1 wpi (Supplementary Fig. S5a). Although BrdU robustly labelled DCX^+ cells after 4 weeks (Supplementary Fig. S5b), $BrdU^+NeuN^+$ cells were again rarely observed at 5 and 9 wpi (Supplementary Fig. S5c,d), indicating that iANBs seldom differentiate into mature neurons under these conditions.

Brain-derived neurotrophic factor (BDNF) and noggin (Nog) have been shown to promote the survival and maturation of neurons originating from the SVZ (refs 48,49). To examine whether these factors can promote the maturation of iANBs, lentivirus expressing BDNF and Nog (BDNF–Nog) under the control of the *hGFAP* promoter was co-injected with SOX2 into the adult mouse striatum. Beginning at 4 wpi, proliferating cells were BrdU-labelled for 4 weeks (Fig. 8a). BDNF–Nog alone was insufficient to induce DCX^+ or $BrdU^+NeuN^+$ cells in the virus-injected striatal region (Fig. 8b). Remarkably, mature $BrdU^+NeuN^+$ neurons were detected in the striatum of mice co-injected SOX2 with BDNF–Nog (Fig. 8b,c).

Valproic acid (VPA), a histone deacetylase inhibitor and common anti-convulsant, promotes normal neurogenesis[50,51]. We tested the effect of VPA on iANB maturation beginning 4 wpi by treating mice twice daily with 150 mg kg^{-1} for 4 weeks. Proliferating cells were simultaneously labelled by BrdU injection (Fig. 8a). As for BDNF–Nog, VPA promoted the appearance of $BrdU^+NeuN^+$ cells in SOX2-injected mice with no effect on mice injected with control virus (Fig. 8b).

Electrophysiology was performed to examine the functionality of astrocyte-derived mature neurons. Although 98% of cells traced by *mGfap–Cre* line 77.6 were astrocytes in the adult striatum, ~0.25% of traced cells expressed NeuN and showed mature neuronal morphology before virus injection. The labelling of resident striatal neurons by this mouse line rendered it unusable for specifically tracing converted mature neurons. In contrast, the *Cst3–CreER^{T2}* line labels astrocytes but not neurons in the adult striatum (Fig. 5); therefore, it was used to examine the electrophysiological properties of iANB-derived neurons. Adult astrocytes and their derivatives were permanently labelled by tamoxifen-induced expression of tdT in *Cst3–CreER^{T2};Rosa–tdT* mice. Two weeks later, SOX2-expressing lentivirus was injected into the adult striatum to reprogram astrocytes to iANBs (Fig. 8d,e). BDNF–Nog-expressing lentivirus was co-injected to promote neuronal maturation. Pilot experiments showed that reprogrammed neurons rarely become electrophysiologically mature before 8 wpi; thus, whole-cell patch-clamp recordings were performed on tdT^+ cells in the adult striatum of live brain slices at 10 wpi or later (Fig. 8e). As DCX^+ iANBs could persist beyond 14 wpi (Fig. 2b), the recorded cells included both immature and mature astrocyte-converted neurons. Some of the recorded cells were also loaded with biocytin, which revealed the elaborate neuronal morphology with spiny or aspiny dendrites (Fig. 8f,g and Supplementary Fig. S6). Most patched cells (13 of 18) exhibited trains of action potentials and large inward currents following depolarization, indicating functional voltage-gated sodium channels (Fig. 8h,i and Supplementary Fig. S7), whereas immature neurons (5 of 18) rarely fired repetitive action potentials or exhibited sodium currents when stimulated (Fig. 8k,l and Supplementary Fig. S7). Resting membrane potential, input resistance, capacitance, action potential threshold, and frequency showed a range of distribution (Supplementary Fig. S8). This might reflect the gradual maturation process of reprogrammed neurons and their intrinsic diversity resembling the heterogeneity observed in endogenous striatal neurons[52,53]. Nevertheless, most of the reprogrammed cells (17 of 18) showed spontaneous synaptic currents indicating the presence of postsynaptic receptors that formed functional synapses with endogenous

striatal neurons (Fig. 8j,m and Supplementary Fig. S7). Together, these data suggested that most of the converted neurons had functionally integrated into the local neural network.

DISCUSSION

Our results demonstrate that the single transcription factor SOX2 is sufficient to reprogram resident brain astrocytes into proliferative neuroblasts in both young adult and aged mice. When treated with neurotrophic factors or a histone deacetylase inhibitor, these astrocyte-converted neuroblasts differentiate into mature neurons and functionally integrate into the local neural network.

SOX2 is a member of the SOXB1 subfamily of high-mobility group box proteins[54] and regulates the self-renewal of both embryonic and adult NSCs (refs 55–58). It plays a key role in reprogramming somatic cells into pluripotent stem cells and NSCs in culture[10–15]. Our present study further demonstrates that SOX2 alone is sufficient to convert resident astrocytes to proliferative neuroblasts in the adult striatum, suggesting that the local microenvironment can facilitate cellular reprogramming. SOX2 is endogenously expressed in certain astrocytes and could be induced by mitogenic and gliogenic signals[59]. We suspect that endogenous SOX2 is insufficient to modulate fate change in astrocytes and that its induction might serve as an early signal for plasticity.

Ectopic SOX2 expression robustly induces iANBs, yet these cells rarely become mature neurons under physiological conditions, suggesting a non-permissive microenvironment. We examined this hypothesis by expressing two candidate factors or treating the mice with a histone deacetylase inhibitor. BDNF, a neurotrophic factor not expressed in the striatum, promotes neuronal differentiation, survival and maturation[60,61]. Nog, a bone morphogenetic protein (BMP) antagonist, promotes adult neurogenesis in the SVZ (ref. 62). Exogenous expression of BDNF–Nog significantly enhances the differentiation of mature neurons from iANBs. The histone deacetylase inhibitor VPA, known to induce BDNF expression[63] and promote neuronal differentiation[50,64], similarly promotes neuronal maturation of proliferating iANBs.

In parallel with previous reports[23–26], this proof-of-principle study demonstrates a feasible strategy for reprogramming somatic cells within adult mammalian tissues. Further studies that aim to identify the extrinsic and intrinsic cues that instruct iANB region-specific neuronal differentiation will be critical to the refinement of this reprogramming technology. Our ability to generate proliferating, non-tumorigenic neuroblasts from resident astrocytes is a milestone in the pursuit of regeneration-based cell therapies for the treatment of CNS-associated injuries or diseases.

METHODS

Animals

Strategies and methods for generating the following transgenic mice have been described previously: *hGFAP–Cre* (ref. 34), *mGfap–Cre* line 77.6 (ref. 35), *Nes–CreER*^{TM} (ref. 33), *NG2–Cre* (ref. 44), *PrP–CreER*^{T} (refs 45,46), *Rosa–YFP* (ref. 65) and *Rosa–tdTomato* (*Ai14*) (ref. 47). *Cst3–CreER*^{T2} mice were generated using the mouse BAC clone RP23-383C3, which encompasses a genomic region 166 kilobases (kb) upstream and 31 kb downstream of the *Cst3* gene. A cDNA containing the coding sequence for *Cre–ERT*^{2} and poly(A) signal was used to replace the ATG start site of the *Cst3* gene through recombination cloning. BAC DNA (50 μg), linearized with the homing endonuclease PI-SceI, was microinjected into the pronuclei of fertilized eggs of FVB/NJ mice. Three founder lines were generated after PCR analysis of genomic DNA from tail biopsies. The transgenic

lines were screened for recombination efficiency after crossing to the *Rosa–YFP* reporter line. No leaky YFP reporter expression was observed in the absence of tamoxifen administration. Wild-type C57/BL6J and ICR mice were obtained from the Jackson Laboratories and Harlan Laboratories, respectively. Aged mice were obtained from National Institute of Aging aged rodent colonies. All mice were housed under a 12 h light/dark cycle and had *ad libitum* access to food and water in the UT Southwestern animal facility. No significant phenotypic differences were observed between male and female mice; thus, both genders were included in the analysis. Mice with ages between 6 weeks and 24 months were used. No statistical method was used to predetermine sample size. The experiments were not randomized. The investigators were not blinded to allocation of animals during experiments and outcome assessment. Experimental protocols were approved by the Institutional Animal Care and Use Committee at UT Southwestern.

Virus production and stereotactic brain injections

The lentiviral vector *hGFAP–GFP* was generated by sub-cloning the synthetic *hGFAP* promoter[31] into the *CS–CDF–CG–PRE* vector with EcoRI and AgeI sites. Candidate genes were then sub-cloned by PCR into the *hGFAP–GFP* vector with AgeI and XhoI sites. Lentiviral *CAG–SOX2* was generated by replacing *hGFAP* promoter with a constitutively active *CAG* promoter from the *Ai9* plasmid[47]. Retroviral plasmid *hGFAP–Cre* was generated by replacing *CAG–RFP* in the retroviral vector *CAG–RFP–WPRE* with *hGFAP–Cre*. Replication-deficient virus was produced in HEK293T (lentivirus) or GP293 (retrovirus) cells by transient transfection. Lentivirus or retrovirus was collected and concentrated by ultracentrifugation (112,000*g* for 2 h at 4 °C) or PEG precipitation[66]. Striata of adult mice were stereotactically injected with a final volume of 2 μl virus each with an original titre of 0.5–2 × 10^9 colony-forming units per millilitre. Viruses were mixed in equal volume for co-injection experiments. Three pools of 12 candidate genes were examined during primary screens: pool 1 (OCT4, SOX2, KLF4 and MYC), pool 2 (ASCL1, BRN2 and MYT1L) and pool 3 (ZFP521, *miR9*, *miR124*, *miR125* and *miR128*). Injection coordinates are as follows: anterior/posterior, +1.0 mm; medial/lateral, ±2 mm; and dorsal/ventral from skull, −3.0 mm. When applicable, mice were bilaterally injected with independent viruses to reduce the total number of animals needed for each experiment.

Tamoxifen and BrdU administration

Tamoxifen (T5648, Sigma) was dissolved in corn oil at a concentration of 20 mg ml^{-1} and injected intraperitoneally at a daily dose of 4 mg per 40 g body weight for the indicated duration. Dividing cells were labelled *in vivo* by intraperitoneal injection of bromodeoxyuridine (BrdU, B5002, Sigma; 100 mg kg^{-1} body weight in PBS, twice daily) or by drinking water containing BrdU (1 g l^{-1}) as indicated.

Immunohistochemistry and quantification

Immunohistochemical analyses of 40 μm brain sections were conducted essentially as previously described[66]. The following primary antibodies were used: GFP (A-11122, rabbit, 1:500, Invitrogen; GFP-1020, chick, 1:1,000, Aves Labs), GFAP (G3893, mouse, 1:500, Sigma), aldolase C (AldoC, SC-12065, goat, 1:200, Santa Cruz Biotechnology), BrdU (rat BU1/75, 1:500, Accurate Chemical), NeuN (MAB377, mouse, 1:500, Millipore), SOX1 (4194S, rabbit, 1:500, Cell Signaling Technology), SOX2 (AB5603, rabbit, 1:500, Millipore), SOX3 (rabbit, 1:200, a gift from M. Klymkowsky[67]), BLBP (AB9558, rabbit, 1:500, Millipore), Ki67 (Ki67P-CE, rabbit, 1:500, Novocastra), DCX (SC-8066, goat, 1:150, Santa Cruz Biotechnology; AB77450, rabbit, 1:500, Abcam), Olig2 (AB9610, rabbit, 1:500, Millipore), S100b (#37, rabbit, 1:1,000, Swant), glutamine synthetase (MAB302, mouse, 1:500, Chemicon), PSA-NCAM (5A5-a, mouse, 1:250, Hybridoma Bank), NG2 (MAB5384,

mouse, 1:500, Millipore), and IBA1 (019-19741, rabbit, 1:1,000, Waco). Alexa Fluor 488-, 594- or 647-conjugated corresponding secondary antibodies from Jackson ImmunoResearch were used for indirect fluorescence. Images were taken using a Zeiss LSM510 confocal microscope. A Cell Counter software plugin in the ImageJ program was used to count cells. Data were obtained from one-sixth of the sections spanning the whole striatal region in each mouse. Animals with failed or mistargeted viral injections were excluded from analysis. A representative image was shown from at least three similar images.

Electrophysiology

Acute sagittal slices covering the striatum were prepared from adult mice (4–8 months old) at 10–21 wpi. For astrocyte recordings, striatal slices were prepared from 6- to 8-week-old mice at 2 wpi. Mice were deeply anaesthetized and transcardially perfused with chilled (4 °C) artificial cerebrospinal fluid (ACSF: 119 mM NaCl, 2.5 mM KCl, 26 mM $NaHCO_3$, 1 mM NaH_2PO_4, 11 mM D-glucose at pH 7.4, 300 mOsm, and aerated with 95% O_2/5% CO_2) including 0.5 mM $CaCl_2$, 5 mM $MgCl_2$ and 1% kynurenate acid. The striatum with overlying neocortex was then dissected out. Acute sagittal slices (250 μm thickness) were collected between ~ + 2 mm and −2 mm from bregma on a Leica VT1200S slicer. Before recording, brain slices were incubated in aerated ACSF with 3 mM $CaCl_2$ and 2 mM $MgCl_2$ for recovery for 30 min at 35 °C, followed by at least 1 h at room temperature. A single slice was then transferred to a submersion chamber and perfused at 3 ml min^{-1} with aerated ACSF at 30 °C. Lineage-traced cells in striatum were identified under visual guidance using IR-DIC optics and RFP fluorescence. Whole-cell current-clamp and voltage-clamp recordings were performed using glass pipettes (~6–9 MΩ) filled with intracellular solution (0.2 mM EGTA, 130 mM K-gluconate, 6 mM KCl, 3 mM NaCl, 10 mM HEPES, 4 mM ATP-Mg, 0.4 mM GTP-Na and 14 mM phosphocreatine-Tris at pH 7.2 and 285 mOsm). For biocytin labelling, intracellular solution was supplemented with 1% biocytin (Sigma, B4261). All recordings were obtained with a MultiClamp 700B amplifier. Currents were filtered at 2 kHz, acquired and digitized at 10 kHz using Clampex10.3 (Molecular Devices). Action potentials were recorded in current clamp mode and elicited by a series of current injections starting from −160 pA with 20, 40, 80 or 160 pA increments and 800 ms in duration. Sodium currents were recorded in voltage clamp mode in response to a series of voltage steps ranging from −60 mV to +60 mV at 10 mV increments and 100 ms in duration. Spontaneous synaptic currents were recorded in voltage clamp mode. In all voltage clamp recordings, cells were clamped at −60 mV or −80 mV, whichever is close to the resting membrane potential of the cell, except during the voltage step protocol. In all current clamp recordings, recordings were made at the resting membrane potential or without any current injection. Series and input resistance were measured in voltage clamp mode with a 400 ms, −10 mV step from a −60 mV holding potential (filtered by 10 kHz, sampled at 50 kHz). Cells were accepted only if the series resistance was less than 40 MΩ and stable throughout the experiment. Data analysis was performed in Clampfit10.3 (Molecular Devices).

Supplementary Material

Refer to Web version on PubMed Central for supplementary material.

Acknowledgments

We thank members of the Zhang laboratory for discussions and reagents. We also thank J. Bibb (UT Southwestern, USA) and P. Chambon (I.G.B.M.C., France) for providing *PrP–CreER*^{T} mice, J. Hsieh (UT Southwestern, USA), C. Kuo (Duke University, USA) and Y. Jan (UCSF, USA) for *Nes–CreER*^{TM} mice, M. Klymkowsky (UC Boulder, USA) for SOX3 antibody, K. Huber for sharing equipment, and E. Olson for critical reading of the manuscript. C-L.Z. is a W. W. Caruth, Jr. Scholar in Biomedical Research. This work was supported by The American Heart Association (09SDG2260602), The Whitehall Foundation Award (2009-12-05), The Welch Foundation Award

(I-1724), The Ellison Medical Foundation Award (AG-NS-0753-11), and NIH Grants (1DP2OD006484 and R01NS070981; to C-L.Z.).

References

1. Zhao C, Deng W, Gage FH. Mechanisms and functional implications of adult neurogenesis. Cell. 2008; 132:645–660. [PubMed: 18295581]
2. Kriegstein A, Alvarez-Buylla A. The glial nature of embryonic and adult neural stem cells. Annu Rev Neurosci. 2009; 32:149–184. [PubMed: 19555289]
3. Ma DK, Bonaguidi MA, Ming GL, Song H. Adult neural stem cells in the mammalian central nervous system. Cell Res. 2009; 19:672–682. [PubMed: 19436263]
4. Hsieh J. Orchestrating transcriptional control of adult neurogenesis. Genes Dev. 2012; 26:1010–1021. [PubMed: 22588716]
5. Kempermann G, Jessberger S, Steiner B, Kronenberg G. Milestones of neuronal development in the adult hippocampus. Trends Neurosci. 2004; 27:447–452. [PubMed: 15271491]
6. Lugert S, et al. Homeostatic neurogenesis in the adult hippocampus does not involve amplification of Ascl1(high) intermediate progenitors. Nat Commun. 2012; 3:670. [PubMed: 22334073]
7. Arvidsson A, Collin T, Kirik D, Kokaia Z, Lindvall O. Neuronal replacement from endogenous precursors in the adult brain after stroke. Nat Med. 2002; 8:963–970. [PubMed: 12161747]
8. Magavi SS, Leavitt BR, Macklis JD. Induction of neurogenesis in the neocortex of adult mice. Nature. 2000; 405:951–955. [PubMed: 10879536]
9. Jablonska B, et al. Chordin-induced lineage plasticity of adult SVZ neuroblasts after demyelination. Nat Neurosci. 2010; 13:541–550. [PubMed: 20418875]
10. Takahashi K, Yamanaka S. Induction of pluripotent stem cells from mouse embryonic and adult fibroblast cultures by defined factors. Cell. 2006; 126:663–676. [PubMed: 16904174]
11. Han DW, et al. Direct reprogramming of fibroblasts into neural stem cells by defined factors. Cell Stem Cell. 2012; 10:465–472. [PubMed: 22445517]
12. Kim J, et al. Direct reprogramming of mouse fibroblasts to neural progenitors. Proc Natl Acad Sci USA. 2011; 108:7838–7843. [PubMed: 21521790]
13. Ring KL, et al. Direct reprogramming of mouse and human fibroblasts into multipotent neural stem cells with a single factor. Cell Stem Cell. 2012; 11:100–109. [PubMed: 22683203]
14. Thier M, et al. Direct conversion of fibroblasts into stably expandable neural stem cells. Cell Stem Cell. 2012; 10:473–479. [PubMed: 22445518]
15. Lujan E, Chanda S, Ahlenius H, Sudhof TC, Wernig M. Direct conversion of mouse fibroblasts to self-renewing, tripotent neural precursor cells. Proc Natl Acad Sci USA. 2012; 109:2527–2532. [PubMed: 22308465]
16. Ambasudhan R, et al. Direct reprogramming of adult human fibroblasts to functional neurons under defined conditions. Cell Stem Cell. 2011; 9:113–118. [PubMed: 21802386]
17. Caiazzo M, et al. Direct generation of functional dopaminergic neurons from mouse and human fibroblasts. Nature. 2011; 476:224–227. [PubMed: 21725324]
18. Heinrich C, et al. Directing astroglia from the cerebral cortex into subtype specific functional neurons. PLoS Biol. 2010; 8:e1000373. [PubMed: 20502524]
19. Heins N, et al. Glial cells generate neurons: the role of the transcription factor Pax6. Nat Neurosci. 2002; 5:308–315. [PubMed: 11896398]
20. Pfisterer U, et al. Direct conversion of human fibroblasts to dopaminergic neurons. Proc Natl Acad Sci USA. 2011; 108:10343–10348. [PubMed: 21646515]
21. Vierbuchen T, et al. Direct conversion of fibroblasts to functional neurons by defined factors. Nature. 2010; 463:1035–1041. [PubMed: 20107439]
22. Karow M, et al. Reprogramming of pericyte-derived cells of the adult human brain into induced neuronal cells. Cell Stem Cell. 2012; 11:471–476. [PubMed: 23040476]
23. Zhou Q, Brown J, Kanarek A, Rajagopal J, Melton D. A *In vivo* reprogramming of adult pancreatic exocrine cells to beta-cells. Nature. 2008; 455:627–632. [PubMed: 18754011]

24. Song K, et al. Heart repair by reprogramming non-myocytes with cardiac transcription factors. Nature. 2012; 485:599–604. [PubMed: 22660318]
25. Qian L, et al. *In vivo* reprogramming of murine cardiac fibroblasts into induced cardiomyocytes. Nature. 2012; 485:593–598. [PubMed: 22522929]
26. Torper O, et al. Generation of induced neurons via direct conversion *in vivo*. Proc Natl Acad Sci USA. 2013; 110:7038–7043. [PubMed: 23530235]
27. Robel S, Berninger B, Gotz M. The stem cell potential of glia: lessons from reactive gliosis. Nat Rev Neurosci. 2011; 12:88–104. [PubMed: 21248788]
28. Sofroniew MV, Vinters HV. Astrocytes: biology and pathology. Acta Neuropathol. 2010; 119:7–35. [PubMed: 20012068]
29. Sofroniew MV. Molecular dissection of reactive astrogliosis and glial scar formation. Trends Neurosci. 2009; 32:638–647. [PubMed: 19782411]
30. Corti S, et al. Direct reprogramming of human astrocytes into neural stem cells and neurons. Exp Cell Res. 2012; 318:1528–1541. [PubMed: 22426197]
31. Lee Y, Messing A, Su M, Brenner M. GFAP promoter elements required for region-specific and astrocyte-specific expression. Glia. 2008; 56:481–493. [PubMed: 18240313]
32. Scott CE, et al. SOX9 induces and maintains neural stem cells. Nat Neurosci. 2010; 13:1181–1189. [PubMed: 20871603]
33. Kuo CT, et al. Postnatal deletion of Numb/Numblike reveals repair and remodeling capacity in the subventricular neurogenic niche. Cell. 2006; 127:1253–1264. [PubMed: 17174898]
34. Zhuo L, et al. hGFAP-cre transgenic mice for manipulation of glial and neuronal function *in vivo*. Genesis. 2001; 31:85–94. [PubMed: 11668683]
35. Gregorian C, et al. Pten deletion in adult neural stem/progenitor cells enhances constitutive neurogenesis. J Neurosci. 2009; 29:1874–1886. [PubMed: 19211894]
36. Bachoo RM, et al. Molecular diversity of astrocytes with implications for neurological disorders. Proc Natl Acad Sci USA. 2004; 101:8384–8389. [PubMed: 15155908]
37. Dutta G, Barber DS, Zhang P, Doperalski NJ, Liu B. Involvement of dopaminergic neuronal cystatin C in neuronal injury-induced microglial activation and neurotoxicity. J Neurochem. 2012; 122:752–763. [PubMed: 22679891]
38. Aronica E, et al. Cystatin C, a cysteine protease inhibitor, is persistently up-regulated in neurons and glia in a rat model for mesial temporal lobe epilepsy. Eur J Neurosci. 2001; 14:1485–1491. [PubMed: 11722610]
39. Yokota O, et al. Amyotrophic lateral sclerosis with dementia: an autopsy case showing many Bunina bodies, tau-positive neuronal and astrocytic plaque-like pathologies, and pallido-nigral degeneration. Acta Neuropathol. 2006; 112:633–645. [PubMed: 17021751]
40. Kettenmann H, Hanisch UK, Noda M, Verkhratsky A. Physiology of microglia. Physiol Rev. 2011; 91:461–553. [PubMed: 21527731]
41. McKhann GM 2nd, D'Ambrosio R, Janigro D. Heterogeneity of astrocyte resting membrane potentials and intercellular coupling revealed by whole-cell and gramicidin-perforated patch recordings from cultured neocortical and hippocampal slice astrocytes. J Neurosci. 1997; 17:6850–6863. [PubMed: 9278520]
42. Ge WP, Miyawaki A, Gage FH, Jan YN, Jan LY. Local generation of glia is a major astrocyte source in postnatal cortex. Nature. 2012; 484:376–380. [PubMed: 22456708]
43. Richardson WD, Young KM, Tripathi RB, McKenzie I. NG2-glia as multipotent neural stem cells: fact or fantasy? Neuron. 2011; 70:661–673. [PubMed: 21609823]
44. Zhu X, Bergles DE, Nishiyama A. NG2 cells generate both oligodendrocytes and gray matter astrocytes. Development. 2008; 135:145–157. [PubMed: 18045844]
45. Weber P, Metzger D, Chambon P. Temporally controlled targeted somatic mutagenesis in the mouse brain. Eur J Neurosci. 2001; 14:1777–1783. [PubMed: 11860472]
46. Hawasli AH, et al. Cyclin-dependent kinase 5 governs learning and synaptic plasticity via control of NMDAR degradation. Nat Neurosci. 2007; 10:880–886. [PubMed: 17529984]
47. Madisen L, et al. A robust and high-throughput Cre reporting and characterization system for the whole mouse brain. Nat Neurosci. 2010; 13:133–140. [PubMed: 20023653]

48. Chmielnicki E, Benraiss A, Economides AN, Goldman SA. Adenovirally expressed noggin and brain-derived neurotrophic factor cooperate to induce new medium spiny neurons from resident progenitor cells in the adult striatal ventricular zone. J Neurosci. 2004; 24:2133–2142. [PubMed: 14999064]
49. Cho SR, et al. Induction of neostriatal neurogenesis slows disease progression in a transgenic murine model of Huntington disease. J Clin Invest. 2007; 117:2889–2902. [PubMed: 17885687]
50. Hsieh J, Nakashima K, Kuwabara T, Mejia E, Gage FH. Histone deacetylase inhibition-mediated neuronal differentiation of multipotent adult neural progenitor cells. Proc Natl Acad Sci USA. 2004; 101:16659–16664. [PubMed: 15537713]
51. Hao Y, et al. Mood stabilizer valproate promotes ERK pathway-dependent cortical neuronal growth and neurogenesis. J Neurosci. 2004; 24:6590–6599. [PubMed: 15269271]
52. Kreitzer AC. Physiology and pharmacology of striatal neurons. Annu Rev Neurosci. 2009; 32:127–147. [PubMed: 19400717]
53. Tepper JM, Tecuapetla F, Koos T, Ibanez-Sandoval O. Heterogeneity and diversity of striatal GABAergic interneurons. Front Neuroanat. 2010; 4:150. [PubMed: 21228905]
54. Chew LJ, Gallo V. The Yin and Yang of Sox proteins: Activation and repression in development and disease. J Neurosci Res. 2009; 87:3277–3287. [PubMed: 19437544]
55. Graham V, Khudyakov J, Ellis P, Pevny L. SOX2 functions to maintain neural progenitor identity. Neuron. 2003; 39:749–765. [PubMed: 12948443]
56. Ferri AL, et al. Sox2 deficiency causes neurodegeneration and impaired neurogenesis in the adult mouse brain. Development. 2004; 131:3805–3819. [PubMed: 15240551]
57. Miyagi S, et al. Consequence of the loss of Sox2 in the developing brain of the mouse. FEBS Lett. 2008; 582:2811–2815. [PubMed: 18638478]
58. Favaro R, et al. Hippocampal development and neural stem cell maintenance require Sox2-dependent regulation of Shh. Nat Neurosci. 2009; 12:1248–1256. [PubMed: 19734891]
59. Bani-Yaghoub M, et al. Role of Sox2 in the development of the mouse neocortex. Dev Biol. 2006; 295:52–66. [PubMed: 16631155]
60. Huang EJ, Reichardt LF. Neurotrophins: roles in neuronal development and function. Annu Rev Neurosci. 2001; 24:677–736. [PubMed: 11520916]
61. Altar CA, et al. Anterograde transport of brain-derived neurotrophic factor and its role in the brain. Nature. 1997; 389:856–860. [PubMed: 9349818]
62. Lim DA, et al. Noggin antagonizes BMP signaling to create a niche for adult neurogenesis. Neuron. 2000; 28:713–726. [PubMed: 11163261]
63. Fukumoto T, Morinobu S, Okamoto Y, Kagaya A, Yamawaki S. Chronic lithium treatment increases the expression of brain-derived neurotrophic factor in the rat brain. Psychopharmacology (Berl). 2001; 158:100–106. [PubMed: 11685390]
64. Hall AC, et al. Valproate regulates GSK-3-mediated axonal remodeling and synapsin I clustering in developing neurons. Mol Cell Neurosci. 2002; 20:257–270. [PubMed: 12093158]
65. Srinivas S, et al. Cre reporter strains produced by targeted insertion of EYFP and ECFP into the ROSA26 locus. BMC Dev Biol. 2001; 1:4. [PubMed: 11299042]
66. Niu W, Zou Y, Shen C, Zhang CL. Activation of postnatal neural stem cells requires nuclear receptor TLX. J Neurosci. 2011; 31:13816–13828. [PubMed: 21957244]
67. Wang TW, et al. Sox3 expression identifies neural progenitors in persistent neonatal and adult mouse forebrain germinative zones. J Comp Neurol. 2006; 497:88–100. [PubMed: 16680766]

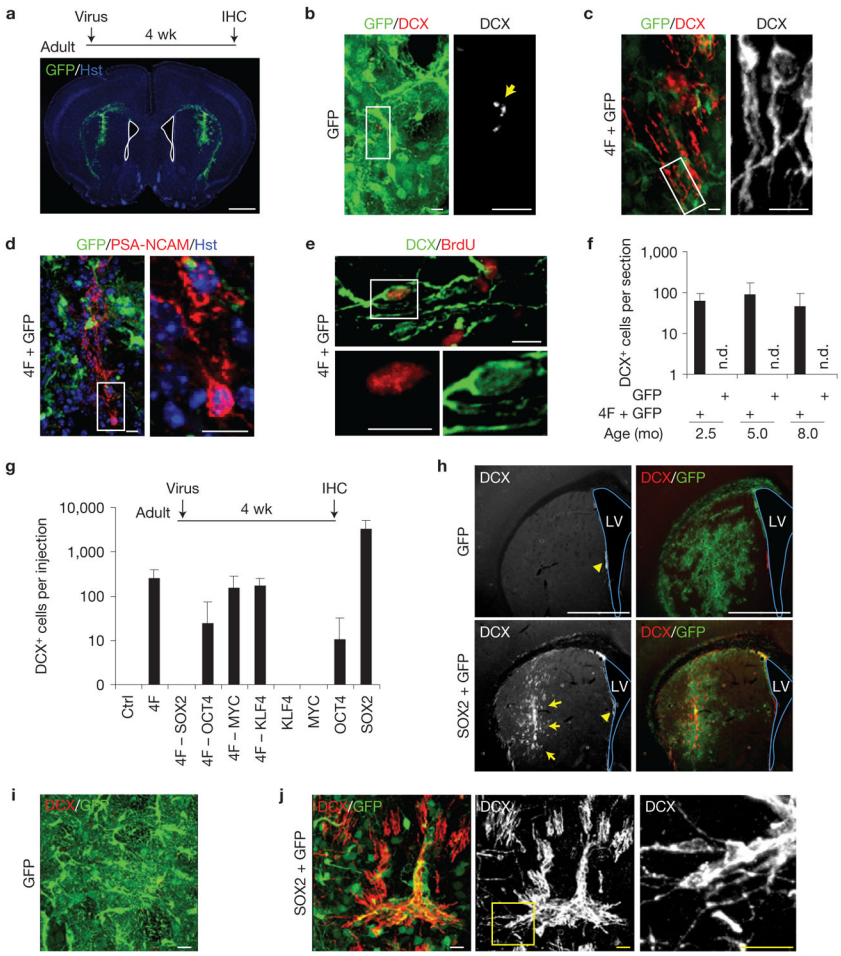

Figure 1.

Inducing *de novo* neurogenesis in adult mouse brains. (**a**) Screening strategy. GFP expression indicates virus-infected striatal regions. Nuclei were counterstained with Hoechst 33342 (Hst). The lateral ventricle is outlined. IHC, immunohistochemistry; wk, weeks. (**b**,**c**) Representative images showing DCX^+ cells in 4F-injected but not in control GFP-injected brains. Nonspecific stains in control brains are indicated by an arrow. (**d**) PSA-NCAM expression in 4F-injected brain regions. Higher-magnification views of the outlined areas are shown in the right panels (**b**–**d**). (**e**) BrdU-labelling shows that DCX^+ cells in 4F-injected areas were newly generated. The bottom panels are higher-magnification views of the outlined area. (**f**) A pool of 4 factors (4F) was sufficient to induce DCX^+ cells in adult mouse brains across three tested age groups, whereas the GFP control had no effect. n.d., not detected; mo, months. Data are presented as mean ± s.d., n = 3, 9 and 5 injections at the age of 2.5, 5 and 8 months, respectively. (**g**) Screens to identify the key factor(s) within the 4F pool. Total DCX^+ cells were counted within the injected striatal regions. Data are presented as mean ± s.d., n = 8 injections for GFP (Ctrl) and 4F, n = 6 injections for 4F– MYC, and n = 4 injections for the remaining experimental groups. (**h**) Low-magnification views of the injected brain regions showing overall expression of GFP and DCX. Arrows show regions with massive SOX2-induced DCX^+ cells, whereas arrowheads indicate endogenous DCX^+ cells near the lateral ventricle (LV). Co-injected GFP shows virus-infected regions. (**i**) A representative image from control GFP virus-injected brain regions. DCX^+ cells were not detected. (**j**) Confocal images showing DCX^+ cells induced by SOX2. The right panel is a

higher-magnification view of the outlined area. Scale bars: 1 mm (**a**,**h**), 20 μm (**i**, **j**) and 10 μm (**b**–**e**).

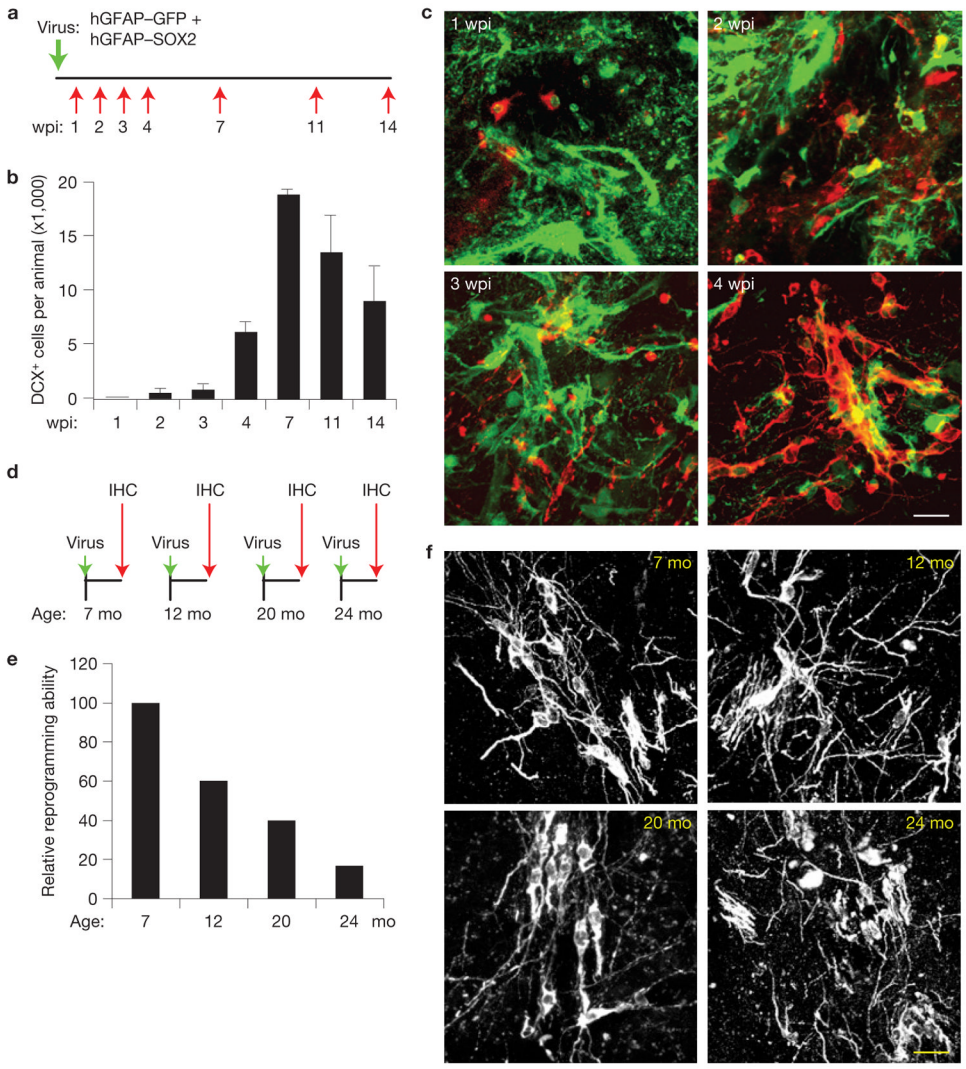

Figure 2.

Progressive generation of iANBs. (**a**) Experimental design to examine the time course of iANB generation. Lentivirus was injected into the adult striatum and analysed at the indicated time points. wpi, weeks post injection. (**b**) Quantification of induced DCX$^+$ cells. Data are presented as mean ± s.d., n = 3 animals at 7 wpi, and n = 4 animals for the rest of time points. (**c**) Immunofluorescence staining of DCX$^+$ cells in virus-injected regions at the indicated wpi. (**d**) Experimental design to examine the effect of age on iANBs. Mice at the indicated ages were injected with SOX2 lentivirus and analysed at 5 wpi. (**e**) The number of SOX2-induced DCX$^+$ cells was quantified and normalized to 7-month-old mice. n = 4 animals at 7 mo, n = 5 animals at 12 and 20 mo, and n = 6 animals at 24 mo. (**f**) Morphology of induced DCX$^+$ cells in virus-injected striatal regions at the indicated ages. Scale bars: 20 μm.

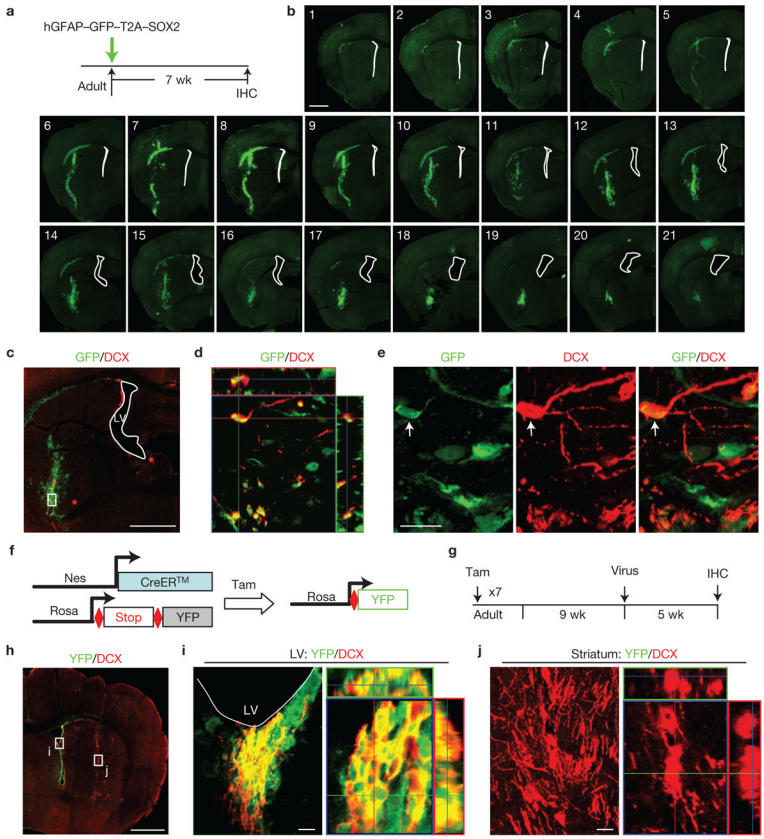

Figure 3.

iANBs are locally produced within the adult mouse striatum. (**a**) Experimental design. Infected cells are marked by co-expressed GFP. (**b**) Serial coronal brain sections spanning the virus-injected regions show that cells within the lateral ventricle (marked by white lines) were not infected by lentivirus. (**c**) A lower-magnification view of virus-infected cells significantly away from the lateral ventricle (LV). Higher-magnification views of the cells in the region outlined by the rectangle are shown in **d**,**e**. (**d**) An orthogonal view of induced DCX^+ cells that co-express GFP, indicating that they are derived from virus-infected cells. (**e**) Higher-magnification views of cells in the region outlined by the rectangle in **c**. (**f**,**g**) A genetic strategy to trace NSCs and their progenies within the adult neurogenic niches. Tam, tamoxifen. (**h**) Lower-magnification views of YFP and DCX expression in lineage-traced and SOX2-virus-injected *Nes–CreER^{TM};Rosa–YFP* mice. (**i**) Confocal analysis showing DCX^+ cells within the lateral ventricle (the outlined region **i** in **h**) are traced with YFP. (**j**) SOX2-induced DCX^+ cells within the injected striatal area (the outlined region **j** in **h**) are YFP^-, indicating that they are locally produced rather than migrating from the endogenous neurogenic niches. Scale bars: 1 mm (**b**,**c**,**h**) and 20 μm (**e**,**i**,**j**).

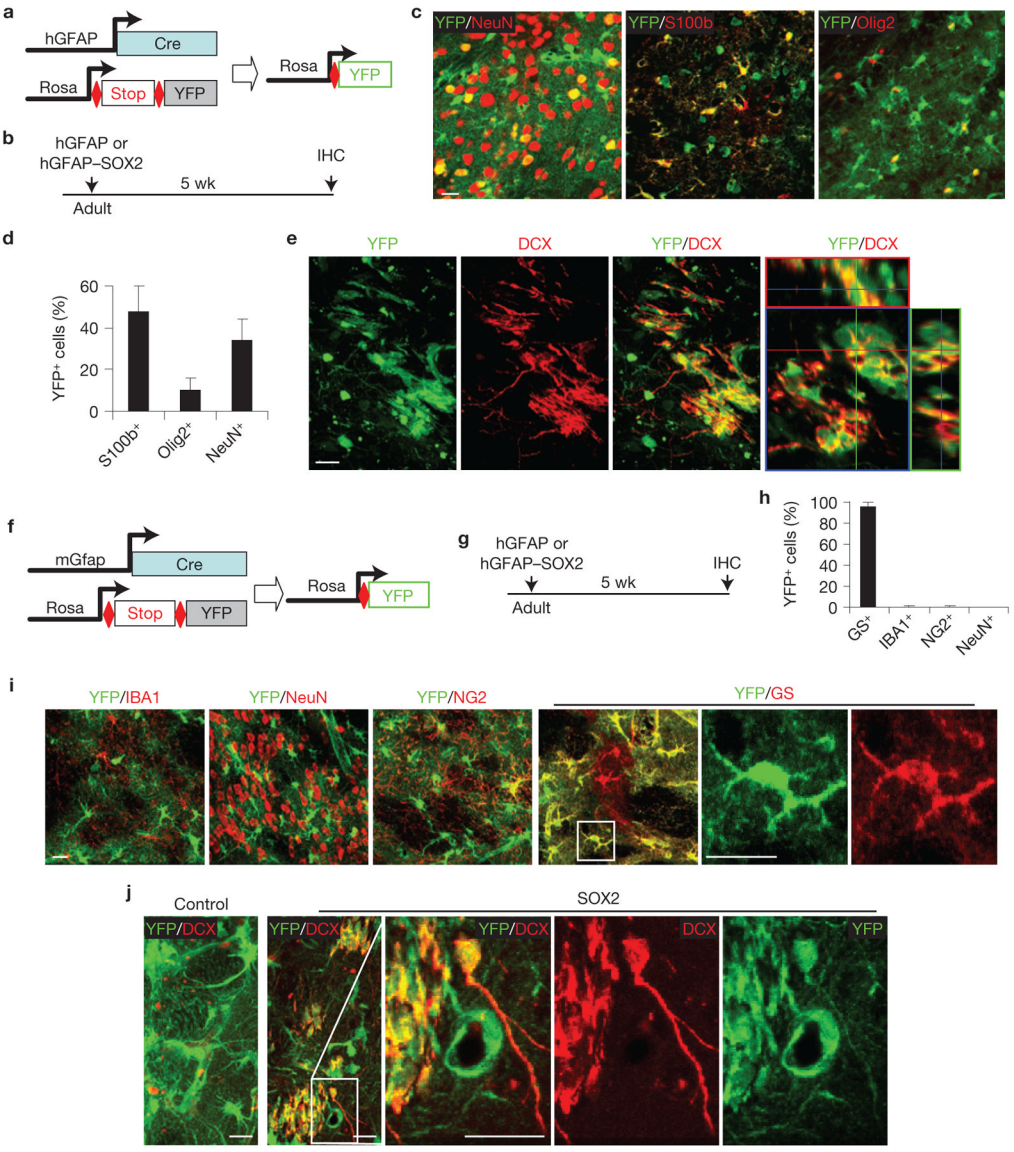

Figure 4.

iANBs originate from cells traced by *hGFAP–Cre* or *mGfap–Cre* line 77.6. (**a**) A genetic approach to trace glial cell lineage using *hGFAP–Cre;Rosa-YFP* mice. (**b**) Experimental design. (**c**,**d**) *hGFAP–Cre* traces astrocytes (S100b$^+$), neurons (NeuN$^+$) and some oligodendrocytes (Olig2$^+$). Data are presented as mean ± s.d. Mean is shown for $n = 3$ animals, scoring for each animal 280 or more YFP$^+$ cells from 3 to 6 brain sections for each marker. (**e**) Immunofluorescence analysis showing that nearly all DCX$^+$ cells are also YFP$^+$ in striatal regions injected with SOX2 virus. (**f**) A genetic approach to trace glial cell lineage using *mGfap–Cre* line 77.6;*Rosa–YFP* mice. (**g**) Experimental design. (**h**,**i**) Most cells traced by *mGfap–Cre* line 77.6 are astrocytes (GS$^+$) and not other cell types. Data are presented as mean ± s.d. Mean is shown for $n = 3$ animals, scoring for each animal 300 or more YFP$^+$ cells from 3 to 6 brain sections for each marker. (**j**) Immunofluorescence analysis showing nearly all DCX$^+$ cells are also labelled by YFP in striatal regions injected with SOX2 virus. Higher-magnification views of the outlined areas are shown in the right panels (**i**,**j**). Scale bars, 20 μm.

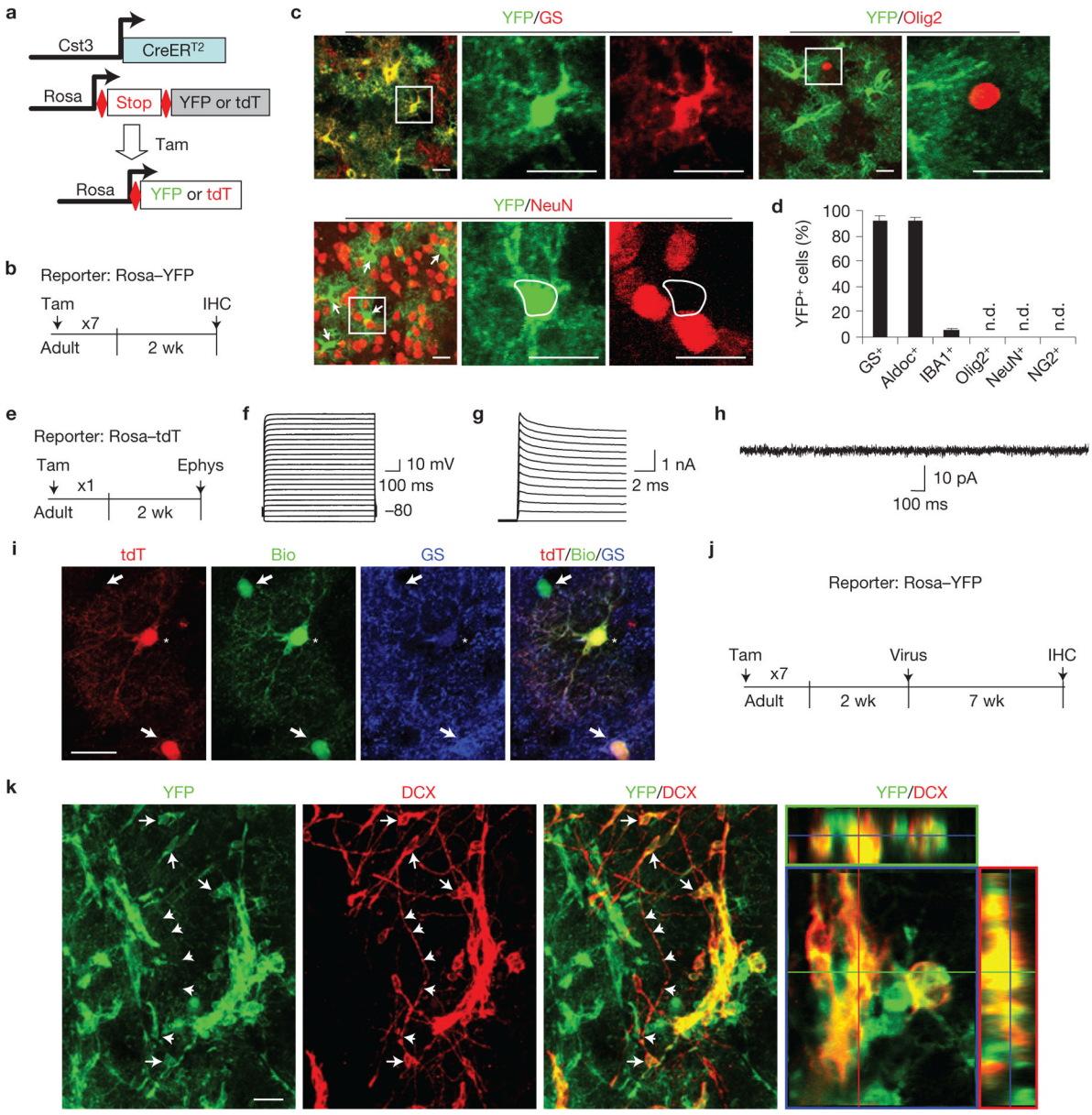

Figure 5.

iANBs originate from astrocytes. (**a**,**b**) A genetic strategy to trace astrocytes and their derivatives. (**c**,**d**) Immunohistochemistry analyses showing that most YFP-traced cells in the adult striatum are astrocytes (GS$^+$ or Aldoc$^+$). Higher-magnification views of the outlined areas are shown in the right panels. n.d., not detected. Arrows show NeuN$^-$YFP$^+$ cells. Data are presented as mean ± s.d. Mean is shown for n = 3 animals, scoring for each animal 250 or more YFP$^+$ cells from 3 to 6 brain sections for each marker. (**e**) An experimental scheme to analyse the electrophysiological properties of *Cst3–CreER^{T2}*-traced cells. Ephys, electrophysiology. (**f**) Voltage responses of a tdT$^+$ cell to current steps from −160 pA with +160 pA intervals. (**g**) Current responses of the same tdT$^+$ cell to voltage steps from −60 mV with +10 mV intervals. (**h**) Current recordings from the same tdT$^+$ cell clamped at −80 mV with no stimulation. (**i**) The recorded tdT$^+$ cell (indicated by an asterisk) was loaded with biocytin (bio). Neighbouring GS$^+$ astrocytes (indicated by arrows) were also bio-

labelled as a result of gap junction coupling between astrocytes. (**j**,**k**) SOX2-induced DCX^+ cells in the striatum are labelled by YFP in *Cst3–CreER^{T2};Rosa–YFP* mice, indicating an origin of astrocytes. Arrows and arrowheads respectively show cell bodies and processes that are positive for both YFP and DCX. Scale bars, 20 μm.

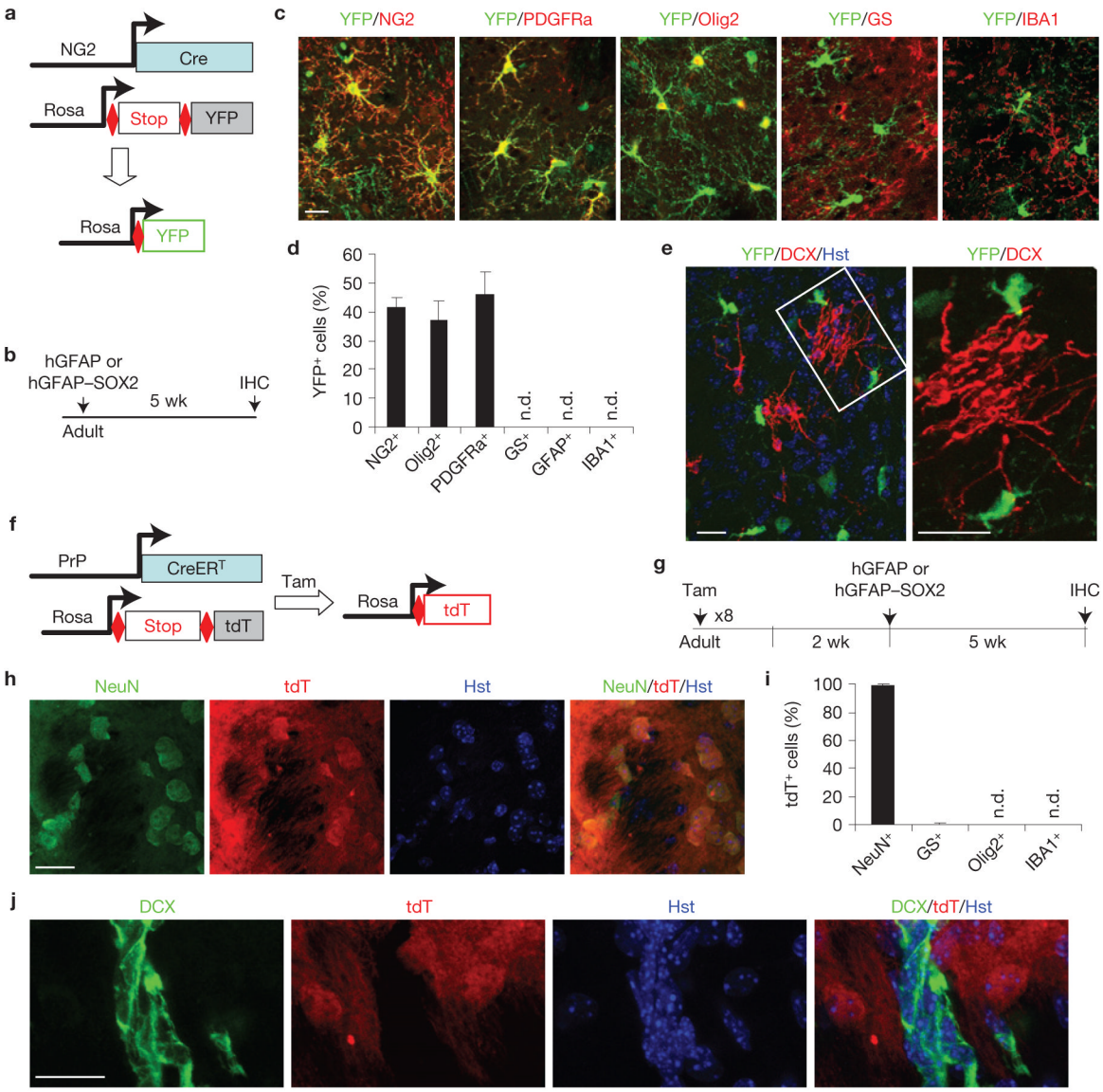

Figure 6.

Neither NG2-glia nor neurons contribute to iANBs. (**a**) A genetic approach to trace NG2-glia lineage. (**b**) Experimental design. (**c**,**d**) *NG2-Cre*-traced cells are NG2 cells, oligodendrocytes or their precursors, but not astrocytes or microglia. n.d., not detected. Data are presented as mean ± s.d. Mean is shown for $n = 3$ animals, scoring for each animal 250 or more YFP^+ cells from 3 to 6 brain sections for each marker. (**e**) Immunofluorescence analysis showing none of the induced DCX^+ cells is labelled by YFP in striatal regions injected with SOX2 virus. A higher-magnification view of the outlined area is shown in the right panel. (**f**,**g**) A genetic approach to trace neurons and their derivatives. (**h**,**i**) Neurons are permanently labelled by tamoxifen induced expression of tdT in *PrP–CreER^T;Rosa–tdT* mice. Data are presented as mean ± s.d. Mean is shown for $n = 3$ animals, scoring for each animal 300 or more tdT^+ cells from 3 to 6 brain sections for each marker. (**j**) SOX2-induced iANBs in the striatum are not labelled by tdT, indicating a non-neuronal origin. Scale bars, 20 μm.

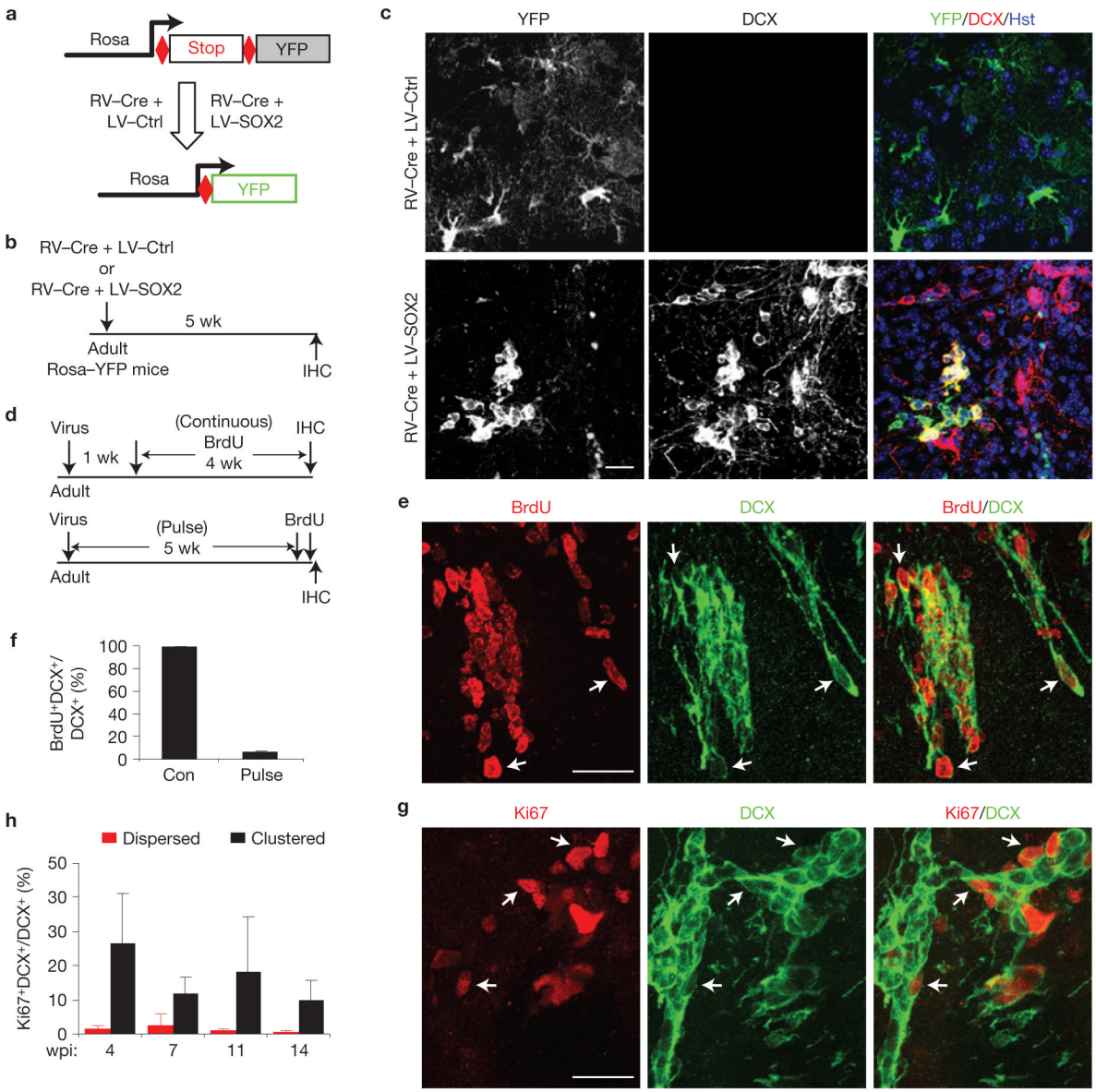

Figure 7.

iANBs pass through a proliferative state. (**a**–**c**) iANBs are largely derived from quiescent glial cells at the time of viral infection. (**a**,**b**) Experimental design. Proliferating cells at the time of viral infection were labelled by retrovirus-expressed Cre (RV–Cre) in *Rosa–YFP* mice. iANBs were induced by lentivirus-expressed SOX2 (LV-SOX2). An empty lentivirus was used as a control (LV-Ctrl). (**c**) Immunofluorescence analysis of DCX^+ and YFP^+ cells in striatal regions. Only 0.9% of DCX^+ cells in SOX2 virus-infected striatal regions are also labelled by YFP. Those rare DCX^+YFP^+ cells are shown. (**d**–**f**) Proliferating iANBs were labelled by either continuous (Con) BrdU-treatment in drinking water for 4 weeks or by 2 pulses of BrdU injections before euthanization. Cells within the virus-injected striatal regions are shown. Arrows indicate co-labelled cells. Data are presented as mean ± s.d., n = 3 and 4 animals for pulse and continuous BrdU-labelling, respectively. (**g**,**h**) $Ki67^+$ cells within clustered or dispersed DCX^+ cells. Arrows indicate co-labelled cells. Data are presented as mean ± s.d. For dispersed cells, n = 8, 4, 4 and 3 animals analysed at 4, 7, 11

and 14 wpi, respectively; for clustered cells, n = 6, 4, 3 and 3 animals analysed at 4, 7, 11 and 14 wpi, respectively. Scale bars, 20 μm.

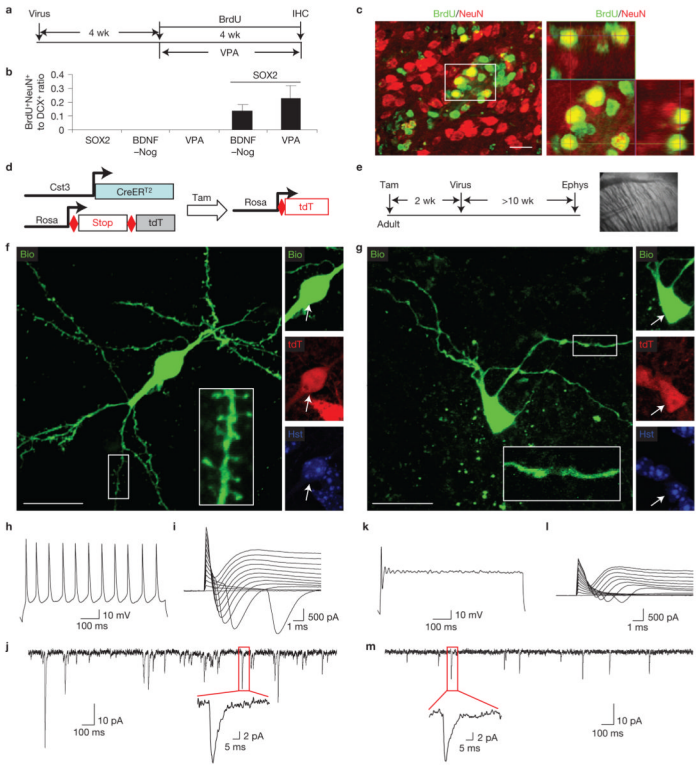

Figure 8.

iANBs develop into functionally mature neurons. (**a**) Experimental design. Adult mice were injected with lentivirus and treated with BrdU for the indicated time period. A separate cohort of mice injected with SOX2 or a control virus was also simultaneously treated with VPA for 4 weeks. (**b**) Quantification of $BrdU^+NeuN^+$ and DCX^+ cells in lentivirus-injected regions. Data are presented as mean ± s.d.; n = 3 and 4 animals for SOX2 + BDNF–Nog and SOX2 + VPA, respectively; n = 5 animals for the remaining groups. (**c**) Immunofluorescence analysis showing $BrdU^+NeuN^+$ cells in regions injected with lentivirus expressing SOX2 and BDNF–Nog. An orthogonal view of the cells in the outlined region is shown in the right panel. (**d**,**e**) Experimental design to analyse the electrophysiological properties of SOX2-induced neurons in the adult striatum. Ephys, electrophysiology. (**f**,**g**) Confocal images of recorded tdT^+ cells (indicated by arrows), which were also loaded with biocytin (Bio) during recording. Enlarged views of the outlined regions show detailed dendritic morphology of the recorded cells. (**h**–**j**) Electrophysiology of a spiny tdT^+ cell labelled in panel **f**. This cell fired repetitive action potentials in response to depolarization (**h**), exhibited inward currents in response to step voltages (**i**), and showed spontaneous synaptic currents when voltage clamped at the resting membrane potential (**j**). (**k**–**m**) Electrophysiological recordings from an aspiny tdT^+ cell labelled in panel **g**. This cell fired a single action potential (**k**), showed smaller inward currents (**l**), and less frequent spontaneous synaptic currents with smaller amplitude (**m**). Scale bars, 20 μm.